



The Solar Probe Plus Ground Based Network

V4.0

November 8, 2015

White Paper Authors: N. A. Schwadron, T. Bastian, J. Leibacher, D. Gary, A. Pevtsov,
M. Velli, J. Burckpile, N. Raouafi, C. Deforest

SPP GBN Committee Members: N. Schwadron (Chair), T. Bastian (Co-Chair),
R. Leamon, M. Guhathakurta, O.C. St. Cyr, K. Korreck, M. Velli, N. Fox, I. Roussev,
A. Szabo, A. Vourlidas, J. Kasper, J. Burckpile, J. Leibacher, S. Habbal, H. Gilbert,
J.T. Hoeksema, T. Rimmele, V. M. Pillet, A. Pevtsov, S. Fineschi, N. Raouafi, D. Gary

Executive Summary. The role of the Solar Probe Plus (SPP) Ground-Based Network (SPP-GBN) is to optimize and enhance the science return of the SPP mission by providing unique data from the ground. The role of the GBN extends to planning and coordination, supported by appropriate infrastructure, to ensure that the right kinds of observations are acquired by the various facilities (see below), at the right times, and that the data are readily accessible to the community for a variety of uses. The SPP-GBN addresses science questions that will help interpreting SPP data, but also provide global context and allow us to understand how SPP observations inform our understanding of solar phenomena. Specifically, the SPP-GBN science questions are

- How do the corona and inner heliosphere magnetically connect to the Sun?
- How are solar energetic particles accelerated and transported to SPP, Solar Orbiter (SO), and other space missions?
- What generates wave and turbulence energy on and near the Sun?

These questions can be traced to GBN measurements, data products, and impacts (see Table 1). This white paper outlines the capabilities of the GBN and the large potential scientific value for the SPP mission.

1 Introduction

The science objectives of the SPP and of the SPP-GBN are related but not identical. The SPP mission has science objectives largely driven by unparalleled opportunities to discover the unexplored environment near the Sun through *in situ* measurements and local imaging of coronal structures. The SPP-GBN provides global context to aid in interpreting the observations delivered by SPP and to enable new science opportunities. In this section we enumerate the SPP Science Objectives and the related supporting Science Objectives of the SPP-GBN. We also present a notional traceability matrix showing the linkages between SPP-GBN science questions and different elements of the GBN.

The document is structured as follows. Section 2 presents the SPP and SPP-GBN Instrumentation and Capabilities, Section 3 the GBN Science Capabilities, Section 4 the Role of the GBN, Section 5 Coordination of the GBN, and the Appendix more detailed specification of some of the capabilities of the Ground Based Facilities

SPP Science Objectives

The primary science objective of the SPP mission is *to determine the structure and dynamics of the Sun's coronal magnetic field and to understand how the corona is heated, the solar wind accelerated, how energetic particles are produced and their distributions evolve*. SPP will achieve this by identifying and quantifying the processes that heat and accelerate the solar wind and solar energetic particles. To advance the

scientific knowledge needed to characterize the inner heliosphere, the SPP mission will address the following overarching science objectives:

- 1. Trace the flow of energy that heats the solar corona and accelerates the solar wind.**
 - 1a. How is energy from the lower solar atmosphere transferred to, and dissipated in, the corona and solar wind?
 - 1b. What processes shape the non-equilibrium velocity distributions observed throughout the heliosphere?
 - 1c. How do the processes in the corona affect the properties of the solar wind in the heliosphere?
- 2. Determine the structure and dynamics of the plasma and magnetic fields at the sources of the solar wind.**
 - 2a. How does the magnetic field in the solar wind source regions connect to the photosphere and the heliosphere?
 - 2b. Are the sources of the solar wind steady or intermittent?
 - 2c. How do the observed structures in the corona evolve into the solar wind?
- 3. Explore mechanisms that accelerate and transport energetic particles.**
 - 3a. What are the roles of shocks, reconnection, waves, and turbulence in the acceleration of energetic particles?
 - 3b. What are the source populations and physical conditions necessary for energetic particle acceleration?
 - 3c. How are energetic particles transported in the corona and heliosphere?

SPP-GBN Science Objectives

Examples of synergetic science enabled by joint SPP and SPP-GBN observations include the following:

- 1- How do the corona and inner heliosphere magnetically connect to the Sun?**
 - a. What is the global context for in situ structures measured by SPP?
 - b. How do transient structures – e.g., CMEs – from the Sun affect the corona and inner heliosphere?
- 2- How are solar energetic particles accelerated and transported to SPP, SO, and other space missions?**
 - a. What are the sources of energetic particle suprathermal seed populations?
 - b. What role do flares and CME-driven shocks play in the acceleration of solar energetic particles?
- 3- What generates wave and turbulence energy on and near the Sun?**
 - a. How does solar wind turbulence evolve between the Sun and SPP?
 - b. What turbulence dissipation mechanism(s) is(are) operative in the corona and solar wind?

Table 1 shows the traceability of these science questions into SPP science questions, GBN capabilities, GBN facilities including coverage, data products, and expected results.

2 SPP and SPP-GBN Instrumentation and Capabilities

2.1 SPP Instrumentation

SPP is comprised of a powerful and complementary suite of four instruments designed to address the fundamental science questions given in Section 1.1 [Fox et al., 2015].

FIELDS, Dr. Stuart D. Bale, PI

The Electromagnetic Fields Investigation (FIELDS; Bale et al. 2015) experiment measures magnetic and electric fields and their fluctuations in situ, and indirectly determines the electron density via plasma noise spectroscopy. The investigation comprises two fluxgate magnetometers (MAG), a search coil magnetometer (SCM) and five electric antennas.

ISIS, Dr. David J. McComas, PI

The Integrated Science Investigation of the Sun energetic particle instrument suite (ISIS; McComas et al. 2014) measures the flux of energetic protons, electrons, heavy ions and their distribution functions (10s of keV to ~100 MeV). The instrument suite comprises two independent instruments (EPI-Hi and EPI-Lo) covering different and overlapping energy ranges.

SWEAP, Dr. Justin Kasper, PI

The Solar Wind Electrons Alphas and Protons Investigation (SWEAP; Kasper et al. 2015) investigation has two electrostatic analyzers (SPAN-A and -B) and a Faraday cup (SPC). This investigation will measure the most abundant particles in the solar wind – electrons, protons and helium ions – and determine their bulk properties such as velocity, density, and temperature and 3D distribution functions.

WISPR, Dr. Russ Howard, PI

The Wide-field Imager for Solar Probe (WISPR; Vourlidas et al. 2015) white-light telescope will take images of the solar corona and inner heliosphere. The experiment will also provide images of the solar wind, shocks and other structures as they approach and pass the spacecraft. This investigation complements the other instruments on the spacecraft providing direct measurements by imaging the plasma the other instruments sample.

HeliOSPP, Dr. Marco Velli, PI

The Heliospheric Origins with Solar Probe Plus (HeliOSPP) PI, Dr. Marco Velli, serves as the Observatory Scientist for the SPP mission, and carries out an interdisciplinary science investigation that focuses on the goals and objectives of the mission. He provides input and independent assessment of scientific performance to the Science Working Group (SWG) and the SPP Project to optimize the scientific productivity of the mission.

2.2 GBN Instrumentation

For now only domestic (U.S.) ground based facilities are listed, mostly those associated with large observatories. It is likely that the list will expand to include additional university-based instruments and it is quite possible that the list will also be expanded to include international partners.

The GBN facilities are extensive. We list these facilities here, and provide definitions and further detail for each in Appendix A.

Optical/infrared (IR) Facilities

- National Solar Observatory - NSO (NISP, DKIST, NISP GONG network, SOLIS)
- High Altitude Observatory – HAO (UCoMP, K-Cor, ChroMag)
- New Jersey Institute of Technology (NJIT) Big Bear Solar Observatory (BBSO; NST, H-alpha, and a GONG station)

Radio Facilities

- National Radio Astronomy Observatory (VLA, VLBA, ALMA)
- NJIT Owens Valley Solar Array (EOVSA)

3. GBN Science Capabilities

3.1 Optical/IR Observations

Optical and IR observations from the ground offer full-sun coverage for mission planning, scientific context, and mapping the origins of the plasma being sampled *in situ* and measured remotely by SPP and SO. “Farside” helioseismic imaging of active regions will support SPP and SO when they are far from the sun–Earth line, and measurements of the Earth-facing hemisphere are otherwise of limited relevance.

Among the phenomena that are important for enhancing SPP–SO science are (1) slowly varying flows of the Sun as a whole (meridional circulation and the torsional oscillation of the fluctuating differential rotation, which are just the latitudinal and longitudinal

components of a vector flow field), which are manifestations of the solar dynamo, and which offer a predicative capability for the long-term variability of the Sun, (2) localized, explosive energy release events (flares, filament eruptions, coronal mass ejections [CMEs]), (3) slower (hours – days) evolution of large-scale structures in the outer solar atmosphere from direct measurements of the magnetic flux and the vector magnetic field, as well as lower atmosphere structures created by these fields (e.g., coronal holes)

The slowly varying fields (1 above) are visible on the surface in Doppler velocity and magnetic-field measurements, and throughout the outer one-third of the solar interior from helioseismology. Explosive energy release (2 above) measurements are available in real-time from 24/7 H α observations and near-real-time magnetic field measurements, as well as in Doppler velocity and helioseismic probes. The development of the instabilities leading to these eruptions is available from helioseismic measures of subsurface flows in active regions, and lower atmosphere measurements of magnetic fields. Helioseismic images of the farside hemisphere of the Sun (invisible to direct measurement from the Earth) will be beneficial for most SPP and SO solar encounters not visible from the Earth. Full-sun and high-resolution magnetic field observations (3 above) are beneficial for understanding conditions at SPP and SO, and their synoptic (slowly varying) view will be important for providing context for all SPP and SO encounters. Campaign observations will be beneficial to support the high spatial resolution objectives.

Dynamic modeling of magnetic field

Following emergence through the photosphere to the corona, magnetic fields experience dramatic changes in (outer) atmospheric conditions (e.g., high-/low- β plasma). These changes lead to a rapid expansion of magnetic flux tubes. The shuffling of different flux systems by plasma motions in the upper convection zone lead to complex topologies of the magnetic field, and the build up of free magnetic energy. This free energy is released to the plasma when relatively confined magnetic flux systems reconnect with larger system(s) of surrounding active regions or even the large-scale coronal fields. These changes are known to affect the temporal evolution of magnetic helicity in emerging active regions (e.g., Longcope & Welsch 2000, Pevtsov, Maleev, & Longcope 2003). They may also result in re-configuration of magnetic connectivity in vicinity of emerging regions, and remote triggering solar eruptions (e.g., Balasubramaniam et al 2011) and flares (e.g., Fu & Welsch 2015). Some studies indicate topological changes in magnetic fields prior to major solar flares (e.g., Burtseva et al. 2015 and references therein). While the changes may appear as “local” in respect to a particular spatial area of the Sun, or a specific height in the atmosphere, they represent a small piece of a much larger process that may span multiple heights and even have an impact on processes in the outer corona and the heliosphere where the SPP measurements will be taken.

To develop a complete understanding of this dynamic evolution of solar magnetic fields one should rely on a combination of (relatively high cadence) observations in the solar

photosphere, chromosphere and corona and modeling. Both high spatial resolution-limited field-of-view and moderate-resolution, large field-of-view observations are important. The former will provide details of the reconnection processes occurring near the reconnection site, and the latter will allow putting the event in the context of a larger picture. Both line-of-sight (LOS) and vector magnetograms can be used in such studies. For example, rapid LOS magnetograms will be useful in detecting early (rapid) changes (emergence) of magnetic field, while the vector data would provide information necessary for in-depth understanding of changes in magnetic energy and helicity, as well as other physical parameters such as Lorentz force. Figure 1 shows example when emergence of a new magnetic flux led to a re-arrangement of existing magnetic topology, which in its turn triggered a CME eruption from a filament channel without filament material. This type of eruptions is associate with so called stealth CMEs (Pevtsov et al 2012).

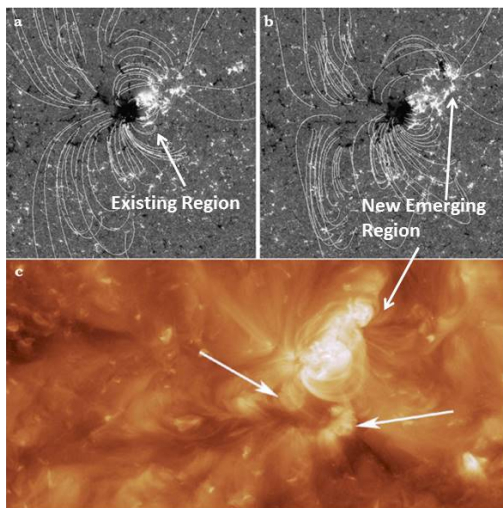


Figure 1: *Evolution of magnetic field leading to change in connectivity of pre-existing magnetic system (upper panel), where the new flux reconnects with field of existing region and opens up magnetic arcade overlying empty filament channel below the active region. While arrows without labels mark bright ribbon-like structures at the base of this magnetic arcade. The origin of stealth CME was triangulated to that location using STEREO A and B observations. Adopted from Pevtsov et al (2012).*

Another example of a data-inspired model is a 3-D MHD simulation by Fan (2011) the drives newly emerging flux at the lower boundary to closely match Hinode soft X-ray observations in magnetic connectivity prior to and throughout the eruption of a magnetic sigmoid into a fast CME. Fan (2011) extends the domain of the model to heights comparable with SPP observations to connect these in-situ data with the magnetic structure of CMEs observed in the low atmosphere.

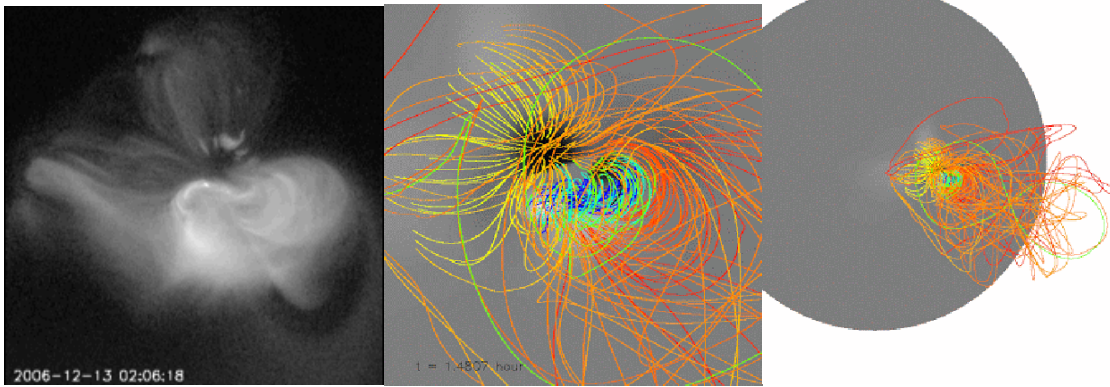


Figure 2: *Far left: Hinode XRT image from Dec 13, 2006 02:06:18 UT just prior to the sigmoid eruption. Center and Right figures show magnetic field simulation of Fan 2011 from a view comparable to Hinode (center) and a view from higher in the corona. Orange field lines outline the region of strong electric current layers.*

Large-scale structure and connectivity

The solar atmosphere is not simply a collection of individual features. It is a single system unified by the presence of large-scale magnetic fields. As a magnetic field feature emerges through the photosphere into the corona, it expands significantly forming a canopy of relatively strong magnetic fields overlying field-free or weaker field areas. X-ray and EUV images show a “network” of loops interconnecting neighboring and distant active regions even across the solar equator (e.g., Pevtsov 2000; Tadesse et al., 2014). In some respects, at any given moment the solar corona is completely filled by the magnetic fields at different scales and field strengths. Because of the $\nabla \cdot \mathbf{B} = 0$ condition, there are no “free” magnetic polarities: every magnetic “pole” is connected to somewhere else. Still, observations show that shortly after its emergence, new magnetic flux establishes new connections with its neighbors, which implies that other previously existed connections would inevitably change. Thus, a seemingly localized flux emergence may lead to readjustment of magnetic topology over much larger area, potentially causing additional heating (e.g., Shibata et al 1991, Pevtsov & Kazachenko 2004, Tarr et al 2015) and/or destabilizing distant coronal flux systems (e.g., Balasubramaniam et al. 2011, Schrijver & Title 2011, Fu & Welsch 2015). In addition to changes in magnetic connectivity, the interaction of pre-existing and newly emerging/evolving magnetic flux systems will lead to a transport of magnetic helicity and energy between magnetic systems on different spatial scales. This helicity and energy transport may affect the stability and physical properties of solar corona on local and global scales. For example, recent studies suggest that magnetic flux systems may contain significant amounts of helicity in their sub-photospheric portions; the helicity in the upper part of a system can then be replenished relatively quickly after a flare or CME eruption and prepare the flux system for the next eruption even without a surface indication of significant build-up of helicity (e.g., Pevtsov 2008 and references therein). Understanding the magnetic

evolution processes that can lead to better prediction of flares and CMEs are critical for advancing solar physics and the practical applications related to space weather at Earth.

Topologies of large- and small-scale magnetic fields may be interlinked. For example, Karachik et al. (2014) have suggested that the formation of (at least some) coronal bright points is governed by the topology of the large-scale magnetic field in the vicinity of bright points.

Nano-flare models of solar wind

The main physical process that is responsible for acceleration of solar wind (SW) remains largely unknown. To date, two major types of models have been proposed to explain the SW acceleration: wave/turbulence-driven models and the reconnection/loop-opening models (e.g., Cranmer et al. 2010; Fisk and Schwadron, 2001; Schwadron and McComas, 2008, Feldman et al., 2005). In wave/turbulence-driven models, photospheric convective flows drive wave-like distortions in the magnetic field. These distortions propagate up into the corona where they dissipate heating the solar corona and accelerating the SW. The presence of Alfvén waves that may be responsible for coronal heating has been reported by Tomczyk et al. (2007). In reconnection/loop-opening models, the SW is “fed” by impulsive bursts associated with the magnetic reconnection between closed and opened magnetic structures. X-ray jets (XRJs) and coronal bright points (CBPs) are usually associated with the reconnection process, and often XRJs and CBPs are also found to correlate with each other. Cirtain et al. (2007) had investigated XRJs in solar polar regions and concluded that the energy flux and mass flow could be sufficient to explain the fast SW acceleration.

Observations by Subramanian et al. (2010) indicate that the interchange reconnection at the boundaries of CHs (Schwadron and McComas, 2005) may act as the driver for slow SW. In contrast, Cranmer & van Ballegoijen (2010) concluded that SW is unlikely to be driven by the reconnection involving the magnetic carpet fields. Karachik & Pevtsov (2011) studied the correlation between fast solar wind (measured in-situ by ACE) and several parameters of coronal holes. They interpreted their results as suggesting that while the reconnection may be a driver for both the slow and fast SW, it is not the primary mechanism for fast SW acceleration. This latter conclusion is in agreement with the Cranmer & van Ballegoijen (2010) arguments based on estimations of energy and timescales for Monte Carlo simulations, which deemed it unlikely that either the slow or fast SW is driven primarily by the reconnection and loop-opening processes at the scale of the “magnetic carpet” fields.

If indeed the reconnection serves as the prime mechanism of fast SW acceleration, one would expect to see a certain correlation between reconnection events in CHs and the properties of fast SW. For instance, CHs with larger numbers of XRJ and CBPs should be associated with stronger SW.

3.2 Radio Observations

For our purposes, radio emission is defined as emission at wavelengths ranging from a few millimeters (≈ 100 GHz) to a few decameters (≈ 10 MHz) – four decades of frequency. The lower frequency boundary corresponds to a frequency cutoff in the ionosphere – radio emission from cosmic sources < 10 MHz cannot propagate through the ionosphere to the ground. However, space based instruments (e.g., ISEE-3, *Wind*/WAVES, *Ulysses*, STEREO/WAVES) can observe ultra-low frequency emission from the outer corona and solar wind. The upper frequency bound is somewhat arbitrary but we use it as a matter of convenience for reasons given below.

Radio Emission from the Sun originates from heights ranging from the low chromosphere up into the corona. A variety of mechanisms produce radio emission:

1. Thermal free–free radiation, produced by collisions of electrons on ions
2. Thermal gyroresonance emission, produced by the gyration of thermal electrons in a (relatively strong) magnetic field
3. Nonthermal gyrosynchrotron emission, produced by nonthermal electrons gyrating in a magnetic field
4. Coherent radio emission, produced by nonlinear interactions between particles and waves (e.g., plasma radiation, cyclotron maser radiation, etc).

Thermal free-free radiation is ubiquitous on the quiet sun. Thermal gyroresonance emission is common in solar active regions whereas nonthermal gyrosynchrotron emission and coherent emissions are associated with transient energetic phenomena such as flares and CMEs. Each of these emission mechanisms provides unique and complementary diagnostics of conditions in the source.

Radio Propagation: Radio emission from objects other than the Sun can be used to study the corona and solar wind. In particular distant background sources – typically quasars – can be used to transilluminate the corona and solar wind. In addition, spacecraft beacons and radar signals have been used in similar fashion. Briefly, turbulence and waves in the corona and solar wind causes a variety of propagation phenomena, referred to collectively as “scattering”, that modify the signal from the distant source. These phenomena include phase scintillations, spectral and angular broadening of the background source or beacon, intensity scintillations, etc.

The breadth of heliophysics that one can address using observations of radio emission is enormous. Here, the SPP-GBN science objectives to which ground based radio facilities can contribute are briefly discussed.

How do the corona and inner heliosphere magnetically connect to the Sun?

Coronal magnetography: Radio observations offer a number of diagnostics that place powerful quantitative and topological constraints on the coronal magnetic field. Briefly, there are:

1. Polarized free-free radiation allows one to measure the line-of-sight magnetic field. It can be used to constrain the field above the limb or on the solar disk.
2. Gyroresonance emission allows one to construct 2D coronal magnetograms in active regions at the base of the corona where the field is force free. Again, measurements can be made above the limb or on the solar disk. The measurements contain intrinsically 3D information. Inversion of the data to constrain the 3D field is a research topic.
3. Mode coupling can be used to place topological constraints on coronal magnetic fields above active regions.
4. Radio bursts can be used to statistically characterize the coronal magnetic field topology from low in the corona to ≈ 2 solar radii.
5. Angular broadening of background sources can be used to measure the orientation of the magnetic field in the plane of the sky from < 2 solar radii to 5 – 10 solar radii. The reason is that turbulence in the inner heliosphere is highly anisotropic. Background sources appear elongated perpendicular to the magnetic field.

Imaging the quiet Sun: The Sun can be imaged at radio wavelengths from chromospheric to coronal heights, revealing macrostructures such as coronal holes and allowing constraints on temperature, density, and magnetic field to be placed on each location and structure.

How are solar energetic particles accelerated and transported to SPP, SO, and other space missions?

Magnetic energy release: new techniques based on dynamic imaging spectroscopy are being developed to probe energy release in X-ray jets and flares. Recent work has used coherent radio emission from type III radio bursts, caused by suprathermal electron beams accelerated by discrete reconnection events; to map beam trajectories from the energy release site. A second example is the identification of a termination shock resulting from a reconnection outflow in a flare that was accompanied by a fast CME. These, and other, techniques are poised to deliver new insights into the location and circumstances of magnetic energy release in the corona and its propagation into the outer corona and solar wind where SPP will be making its measurements.

Particle acceleration and transport: while coherent plasma radiation is proving to be an effective tracer of energy release sites and shocks, incoherent gyrosynchrotron radiation – from electrons with energies of 100s of keV to ≈ 10 MeV is effective for measuring the

electron distribution function and its spatiotemporal evolution in the source. It is also effective for measuring coronal magnetic fields in flaring loops.

Coronal mass ejections: certain fast CMEs have been imaged at meter wavelengths, emitting synchrotron radiation from MeV electrons entrained by the CME magnetic field. The details of the spectrum and its spatial and temporal evolution allow measurements of the CME magnetic field and electron number density to be made out to several solar radii.

Coronal shocks: fast CMEs can drive coronal and interplanetary shock. Ground based radioheliographs can image the formation and propagation of shocks using type II radio bursts as proxies of coronal shocks.

What generates wave and turbulence energy on and near the sun?

Scattering phenomena: By studying scattering phenomena, powerful constraints can be placed on turbulence and waves in the corona and solar wind. Among the parameters that can be measured toward a given background sources located at some solar elongation and position angle: the power law index of the spatial spectrum of electron density variations at a wide range of scales; the inner scale of the turbulence; the degree of anisotropy; and the orientation of the magnetic field. By observing many background sources, a map of these quantities can be constructed as a function of radius and position angle. The solar wind speed can be mapped as a function of radius and position angle. It is also the case that such techniques can be used to constrain the properties of transients such as CMEs propagating out into the IPM as they occult background radio sources.

4. The Role of the GBN

Above all, the role of the GBN is to optimize and enhance the science return of SPP and SO by providing unique data from the ground. To do so, however, the role of the GBN also extends to planning and coordination, supported by appropriate infrastructure, to ensure that the right kinds of observations are acquired by the various facilities (see below), at the right times, and that the data are readily accessible to the community for a variety of uses. Therefore, in addition to addressing SPP-GBN science objections, the GBN will optimize SPP science return by playing a central role in the following:

4.1 Monitoring Observations

Reliable monitoring observations, preferably on a 24/7 basis, may be used to understand conditions on the sun and inner heliosphere at any given time during the mission: the structure and evolution of features on the Sun, in the corona, and in the heliosphere – e.g., active regions, coronal holes, filaments, prominences, coronal cavities, streamers, etc..

They will also monitor transient events such as flares and CMEs and their properties. Monitoring observations would presumably involve a subset of ground-based facilities that can provide a reliable suite of data types and coverage, the details of which are TBD.

4.3 Forecasting

Monitoring data will be used for providing scientific context for SPP observations. They will also play a role in forecasting conditions on the Sun and in the heliosphere on a variety of time scales.

4.4 Modeling

Monitoring data will be necessary for certain types of modeling whereas campaign observing will be used for others. Modeling will play a central role in realizing SPP-GBN science objectives as well as in forecasting and mission planning.

4.5 Mission Planning

Mission planning will benefit from “situational awareness” for conditions on the Sun and in the heliosphere. Data-driven models can enable reliable forecasts of conditions during various phases of the mission.

5 Coordination of the GBN

GBN facilities will significantly enhance SPP and SO science returns. The primary challenge is in organizing and coordinating GBN participation in both routine and critical phases of the SPP and SO missions. We have summarized U.S.-based assets here. The GBN should be internationalized to ensure maximum ground based coverage for SPP and SO. Detailed plans are not developed here, however. We simply summarize some considerations looking forward.

5.1 Types of observing support

The various types of observing support must reflect SPP-GBN needs to address the relevant science objectives, as well as the availability of various facilities. Many facilities in the U.S. are national observatories that serve broad communities. Specific programs will likely need to be implemented to support SPP. For example, the VLA and VLBA of the NRAO are PI instruments that receive ≈ 1000 proposals annually. It may be necessary to develop an MoU between NASA and the NRAO to ensure availability to these instruments during critical phases of the mission. There are precedents for this: NASA has come to the NRAO for support of some of its planetary missions. The NSO/DKIST

will operate similarly. The NSO/NISP operates synoptically, but coordination is nevertheless essential to ensure that vital data during SPP and SO encounters are obtained. University-based facilities such as NJIT's BBSO and EOVS have fewer such constraints but they, too, may need agreements in place to ensure the reliable delivery of key data products.

Two broad types of GBN observations will be used in coordination with SPP and SO:

- *Monitoring observations* that provide a routine suite of data products that can be used for modeling, forecasting, mission planning, and context. The minimum suite of observations and associated data products must be defined.
- *Campaign observations* that deploy a broader, more diverse suite of instruments that are not necessarily otherwise available to address specific SPP-GBN scientific objectives during critical phases of the mission.

5.2 Data Archiving, Formats, Standards

To facilitate rapid and reliable exchange of GBN data, the SPP-GBN will need to come to agreement on what data formats to support, the meta-data used to describe available data, where to make the data available in real time and near-real time, archive the data, and what tool(s) can be used to access them. A great deal of work has been done in these areas (e.g., Virtual Solar Observatory and various mission archives) and so we would not be starting from scratch. Again, it is a matter of planning and coordination plus some possible development.

5.3 Community Tools

Community software packages, such as FORWARD (Gibson 2015) and GX Simulator (Nita et al. 2015) are currently available that provide a direct comparison between models and data with particular emphasis on coronal magnetic fields and plasma properties. The FORWARD package is a SolarSoft IDL (<http://www.hao.ucar.edu/FORWARD/>) package that interfaces with the Potential Field Source Surface Model, the Magnetohydrodynamics on a Sphere (MAS)-model and other analytic MHD models as well as data provided by missions such as NASA AIA, LASCO and Mauna Loa observations. The package is currently being updated to handle adaptive mesh grids for easier comparison of model extrapolations with SPP in-situ measurements. GX Simulator, also a SolarSoft IDL package (https://web.njit.edu/~gnita/gx_simulator_help/), is a tool for creating 3D active region and flaring loop models, calculating radio, X-ray, and EUV emission from them, with rich tools for intercomparison of models with observational data.

5.4 Scheduling support

There will need to be close coordination between SPP and the SPP-GBN to successfully plan and execute monitoring and campaign observations. The mechanisms for doing so are TBD.

Appendices

A. Ground Based Facilities

A.1 Optical/IR Facilities

National Solar Observatory (NISP, DKIST)

The **NSO Integrated Synoptic Program** (NISP) operates a suite of instruments from the **Global Oscillation Network Group** (GONG) and the **Synoptic Optical Long-term Investigations of the Sun** (SOLIS) programs.

GONG is a network of six identical instruments located at Big Bear Solar Observatory (California), Mauna Loa Observatory (Hawaii), Learmonth Solar Observatory (Australia), Udaipur Solar Observatory (India), Observatorio del Teide (Canary Islands), and Cerro Tololo Interamerican Observatory (Chile), and NISP/GONG data products include full disk 2.5-arcsecond pixel velocity, intensity, and magnetic-flux images of the sun every minute, with an approximate 90% duty cycle, enabling continuous measurement of local and global helioseismic probes from just below the visible surface to nearly the center of the sun. High-cadence, high-sensitivity magnetograms, near-real-time seismic images of the farside of the sun, and $2\text{ k} \times 2\text{ k}$ H α intensity images obtained at a 20-second cadence are also available. Currently, H α intensity images are taken in the core of the line, but it is likely that by SPP launch time the H α instruments will be upgraded by tunable H α filter; at that time images in line core and wings (plus Doppler velocity maps) will be available. Derived data products include classical and synoptic maps of radial magnetic flux, synoptic maps of subphotospheric flows and several models based on PFSS extrapolation: predicted coronal holes, top/ecliptic plane view of extrapolated magnetic fields etc. USAF ADOPT model results based on GONG and SOLIS magnetograms will also be available from the NSO.

SOLIS is composed of a single equatorial mount carrying three telescopes: a 50 cm **Vector Spectromagnetograph** (VSM), a 14 cm **Full-Disk Patrol** (FDP), and an 8 mm **Integrated Sunlight Spectrometer** (ISS). Currently, SOLIS operates in a temporary location in Tucson, Arizona. In 2016 it will be moved to a permanent (still undecided) location. Potential sites for future SOLIS operations include the following geographic areas: US (California, Hawaii, New Mexico). Two candidate sites for future SOLIS operations include the Big Bear Solar Observatory in California and the Sacramento Peak Observatory in New Mexico.

Current NISP/SOLIS data products include daily full disk line-of-sight photospheric (Fe I 6302Å) and chromospheric (Ca II 8452 Å) magnetograms, full vector photospheric magnetograms (Fe I 6302 Å), full disk Doppler and equivalent width “maps” of the sun

in H α and He 10830, coronal hole maps, and sun-as-a-star spectral observations in several spectral bands spanning the low solar atmosphere. Recent upgrade expands SOLIS/VSM capabilities to full disk vector magnetograms in Ca II 8542 chromospheric spectral line. This new data product is currently under development, and is expected to be available soon. In addition, the VSM magnetograms are used to derive classical synoptic maps (radial or line-of-sight component of magnetic field), synoptic maps of vector field (three components), and synoptic maps of uncertainties in radial magnetic flux (the uncertainties are used in ensemble modeling to derive uncertainties in extrapolated (coronal) magnetic field and predicted solar wind parameters).

The FDP is a full-disk imager that uses tunable Lyot filters and a 2048 \times 2048 CCD camera (about 1 arcsecond pixel size). The plan is to take observations with high temporal cadence (about ten seconds) in several (up to eight) selected spectral lines including H α , Ca II K, He I 10830 Å, blue and red continuum (white light), and photospheric lines, as well as Doppler velocity maps in selected lines (most likely, H α).

ISS obtains high spectral resolution ($R = 300,000$) observations of the sun as a star (e.g., for solar irradiance measurements). Currently, ISS takes data in 9 spectral bands: CN band (3884.0 Å), Ca II K (3933.7 Å), Ca II H (3968.5 Å), C I (5380.0 Å), C I (with iodine spectra imposed), Mn I (5394.1 Å), Na D1 (589.59 nm), H α (656.30 nm), Ca II (8541.9 Å), He I (10830.2 Å). Additional spectral bands can be added if needed. The bandwidth varies from about 5.3 Å (CN band) to 16.5 Å (He I). ISS data are taken daily, but the data can be taken continuously through the day (e.g., in a flare mode).

The **Daniel K. Inouye Solar Telescope** (DKIST) is a 4-meter solar telescope located on Maui, Hawaii. It will provide polarimetry of structures of about 20 – 30 km in size over a limited field of view (about 300 arcseconds) from the visible to near and thermal IR. First light instruments include: the **Visible Broadband Imager** (VBI), the **Visible Spectro-Polarimeter** (ViSP), the **Diffraction-Limited Near-Infrared Spectropolarimeter** (DL-NIRSP), the **Cryogenic Near-Infrared Spectropolarimeter** (Cryo-NIRSP), and the **Visible Tunable Filter** (VTF).

The VBI will be able taking high cadence images simultaneously in two spectral bands (blue and red): 393.3 nm – 486.4 nm (VBI blue channel) and 656.3 nm – 705.8 nm (VBI red channel).

- Optical field of view: ≈ 120 arc seconds; physical FOV will be limited by the size of CCD camera (about 45/69 arcsec square for the blue/red channel).
- Spatial resolution: 0.022 arcsec @ 430.5 nm (blue) and 0.034 arcsec @ 656.3 nm (red).
- Spatial sampling: 0.011 arcsec/pix @ 430.5 nm (blue), 0.017 arcsec/pix @ 656.3 nm (red).

- Cadence: 3.2 seconds cadence for reconstructed images with same physical FOV at single or multiple wavelengths
 - 0.033 seconds cadence for raw images with same physical FOV at single wavelength;
 - 0.366 seconds cadence for single images with same physical FOV at multiple wavelengths.

ViSP will provide precision measurements of all four Stokes parameters I , Q , U , and V simultaneously at diverse wavelengths in the visible spectrum, and fully resolving (or nearly so) the spectral profiles of spectral lines originating in the solar atmosphere. Such measurements provide quantitative diagnostics of the magnetic field vector as a function of height in the solar atmosphere, along with the associated variation of the thermodynamic properties. Furthermore, information about protons and electrons in flares can be deduced from analyzing the polarization of strong lines during flares.

- Wavelength range: 380–900 nm; up to three lines simultaneously.
- Spatial resolution: $2 \times$ DKIST resolution or 0.07 arcsec at 630 nm.
- Spatial FOV: 120×120 arcsec.
- Simultaneous operation with: VBI, DL-NIRSP, VTF.

DL-NIRSP is designed to study solar magnetic fields at high spatial resolution with high spectral resolution and polarimetric accuracy.

- Simultaneous spectral coverage: 3 spectral windows; one from each pre-defined band.
 - IFU formats: 80×60 (36 μm pixels); or 60×40 (72 μm pixels) (selectable).
- Spatial resolution: From diffraction limited at 900 nm to 0.5 arcsec sampling (selectable).
- Spectral resolution: $R \approx 70000$ or $R \approx 250000$ (selectable).
- Velocity coverage (Doppler shifts): Up to 240 km/s.
- Polarimetry: Either Full Stokes polarimetry (I, Q, U, V) or Intensity only. Field-of-view: Up to 120×120 arcseconds
- Simultaneous operations with: VBI, VISP, VTF.

Cryo-NIRSP will study the solar coronal magnetic fields over a large field-of-view at near- and thermal-infrared wavelengths. Cryo-NIRSP will measure the full polarization state (Stokes I , Q , U and V) of spectral lines originating on the sun at wavelengths from 1000 nm (500 nm goal) to 5000 nm. It is the only DKIST instrument with the capability of sensitively imaging the relatively faint infrared corona and the thermal infrared solar spectrum. Cryo-NIRSP depends on the full coronagraphic capabilities of DKIST to observe both the near-limb (using DKIST's prime-focus and secondary occulter) and the more distant corona and heliosphere. Its thermal infrared capabilities allow sensitive

study of the solar disk in the CO lines. Near-limb capabilities allow unique observations of spicules, prominences, flares, and eruptive events in the low corona.

- Spectral coverage from 1000 nm to 5000 nm.
- Spectral resolution:
 - 30,000 for coronal observations,
 - 100,000 for disk observations.
- Spatial resolution:
 - 0.5 arc second/pixel size for coronal observations,
 - 0.15 arc seconds sampling for disk observations (at 4.7 micron).
- Field of View:
 - Coronal mode 4 arc minutes parallel to the limb, 3 arc minutes perpendicular to the limb;
 - Disk mode, 1.5 arc minutes square.
- Multiple wavelengths: observable at high efficiency.
- Context imager: will sample the coronal field of view with ≤ 0.5 arc seconds per pixel.

The VTF is designed to spectrally isolate narrow-band images of the sun at the highest possible spatial and temporal resolution from the DKIST telescope. The instrument will allow taking 2D spectral data, Doppler velocity maps, transverse flows, and maps of the magnetic field components on spatial scales between 20 km and 40000 km.

- Spectral Range: 520 nm to 870 nm.
- Spectral resolution: 6 pm (@600 nm).
- Spectral sampling: 3 pm (@600 nm).
- Field of view: 60" \times 60".
- Spatial Sampling: 0.014 arcsec/pixel.

High Altitude Observatory (UComp, K-Cor, ChroMag)

The **Coronal Multi-Channel Polarimeter** (COMP) infers information about the coronal magnetic field by measuring the polarization of light from the corona and prominences in the forbidden emission lines of Fe XIII at 1074.7 nm and 1079.8 nm as well as the emission line at 1083.0 nm produced by neutral Helium. CoMP records the total intensity and the linear and circular polarization of light (Stokes I , Q , U , V) at all three wavelengths and combines like polarization states and wavelengths to produce calibrated images with a nominal time cadence of 30 seconds at 9 arcsec spatial resolution (4.5 arcsec pixels). Observations of these linear polarization states provide information about the direction of the coronal magnetic field in the observer's 'plane-of-the-sky' (POS), but do not provide information on the strength of the field in this plane. This sensitivity to field direction arises from the fact that the polarization is produced by resonance scattering of photospheric radiation from coronal electrons. The direction of the resulting

linear polarization is changed in the presence of a magnetic field, with the polarization aligned with or perpendicular to the direction of the magnetic field. Because the natural line widths of these forbidden lines are very small compared with the Zeeman splitting under coronal conditions, the scattering radiation is no longer sensitive to the strength of the magnetic field. CoMP Doppler observations of wave speeds in the corona can provide constraints on the magnitude of the magnetic field in the sky plane. Information about the strength of the magnetic field in the observer's direction is directly provided via the circular polarization through the longitudinal Zeeman effect.

The CoMP instrument upgrade (UCoMP) will be completed by 2018 via funding from NSF and NCAR/HAO. The upgrade will greatly expand the number of observed wavelengths and will include the installation of a second camera to provide better spatial resolution and larger field-of-view. These upgrades will provide new observations of the coronal magnetic field in cooler coronal regions (e.g. Fe X, Fe XI) where the solar wind escapes as well as in hotter emission lines (up to 7 million degrees K, e.g. FeXIV) regions to study solar flares. The bulk of the proposal support from NSF is going to the University of Michigan (P.I.: Dr. Enrico Landi) to create a joint data distribution and analysis center for the Heliophysics community.

The COSMO **K-Coronagraph** (K-Cor) records the linear polarization of photospheric radiation Thomson-scattered by coronal electrons in a 30 nm bandpass centered on 730 nm. K-Cor is an internally occulted refracting coronagraph with 5.5 arcsec pixels and a nominal cadence of 15 seconds that provide unique high time cadence white light images of the very low corona (1.05 to 3 R_{\odot}) where CMEs form. These observations compliment space-based coronagraphs such as LASCO and STEREO and emission observations of the corona from SDO.

The COSMO **Chromospheric Magnetometer** (ChroMag) is scheduled for deployment to MLSO in 2016. ChroMag will acquire full-disk spectro-polarimetric images of the sun in a variety of wavelengths including Helium-I 587.6 and 1083.0 nm, Ha 656.3 nm, Ca II 854.2 nm and Fe I 617.3 nm. All wavelengths will be acquired in less than one minute with 2 arcsec spatial resolution. ChroMag will provide full-vector chromospheric and photospheric magnetograms, dopplergrams, and high time cadence imagery of chromospheric dynamics. This new capability will enhance our understanding of how energy is transported into the corona and how the solar wind is accelerated. ChroMag observations will capture the dynamical interaction between the magnetic field and plasma of filament and prominence eruptions, which is important for realtime space weather forecasting of coronal mass ejections (CMEs). ChroMag will produce 400 GB / hour which is 20 times as much as MLSO current generates in 1 hour. HAO is working with the community to identify observing modes that are most conducive to discovery science.

NJIT Big Bear Solar Observatory (BBSO)

The Big Bear Solar Observatory is the site of the high-order adaptive-optics (AO)-corrected NST and its post-focus instrumentation (which consists of a broadband filter imager—BFI; visible imaging spectrometer—VIS; near-infrared imaging spectropolarimeter—NIRIS; fast-imaging solar spectrograph—FISS; and a cryogenic infrared spectrograph—Cyra). Also on the site is an H α full-disk imager (part of the Global H α Network) and a Global Oscillation Network Group (GONG) station.

BBSO NST Instrumentation

NST High-Order and Multi-Conjugate Adaptive Optics

The AO-308 system, with its 308 sub-apertures, provides high-order correction of atmospheric seeing within an isoplanatic patch (about 6" at 500 nm in summer), with a gradual roll-off of correction at larger distances. We are developing a new system called Multi-Conjugate Adaptive Optics (MCAO), using two deformable mirrors that can correct turbulence at two layers simultaneously—the ground layer at < 500 m, and the boundary layer at 3-6 km. This system will be operational within a year or two, and can be expected to provide diffraction-limited correction over a much wider area of the image in the era of Solar Probe Plus and Solar Orbiter. The diffraction limit of a 1.6 m telescope is 0.08" at 500 nm, and 0.16" at 1 micron.

NST Broad-Band Filter Imager—BFI

The broad-band filter imager provides continuum context data over an AO-corrected field using a high-speed 2048x2048 CCD camera. Two bands currently used are G-band (430.5 nm, 5-Å bandpass) with a field of view of 55" and 0.027"/pixel image scale, and TiO (705.7 nm, 10-Å bandpass) with a field of view of 70" at 0.034"/pixel image scale. Filtergrams are typically taken in short bursts of 100 frames every 15 s, and processed via speckle reconstruction to achieve diffraction-limited images (resolutions of 0.06" in G-band, 0.09" in TiO).

NST Visible Imaging Spectrometer—VIS

VIS currently uses a single Fabry-Pérot etalon to produce a narrow 0.07-Å bandpass over a 70" circular field of view, tunable from 550-700 nm. Plans are underway to upgrade VIS to a dual-etalon system. Available spectral lines include H α , Fe I 630 nm, and Na I D2 (589 nm). Plans are underway to add the He I D3 line. The image scale is 0.034"/pixel, and typically 11 line positions are sampled in 15 seconds, although the number of line positions (and corresponding time resolution) is a settable parameter. Bursts of typically 25 frames are used for speckle reconstruction at each line position. The purpose of VIS is to provide spectral diagnostics of solar features at the diffraction limit of the telescope.

NST Near Infra-Red Imaging Spectropolarimeter—NIRIS

NIRIS uses dual Fabry-Pérot etalons that provide an 85" round field of view. The BBSO has just brought into use a new Teledyne camera, a 2024 × 2048 HgCdTe, closed-cycle He cooled IR array. The system utilizes half the chip to capture two simultaneous polarization states side-by-side, each 1024 × 1024 pixels in size, providing an image scale of 0.083"/pixel. The other half of the chip will be used in the future for two out-of-focus images to be used for phase-diversity correction. The primary lines used by NIRIS are the Fe I 1565 nm doublet, and the He I 1083 nm multiplet. The Fe I bandpass is 0.1 Å while the He I bandpass is 0.05 Å. The polarimetry is done via a rotating waveplate that samples 16 phase angles at each line position, and more than 100 line positions at a cadence of 10 seconds per full spectroscopic measurement (full-Stokes I , Q , U and V). The inversion of these data to provide magnetograms and other spectral diagnostics is currently under development. The system can also be operated in a fixed-phase-angle, dual-polarization mode that would allow speckle reconstruction of I and V images for diffraction-limited line-of-sight magnetic field diagnostics.

NST Fast-Imaging Solar Spectrograph—FISS

FISS is a scanning Echelle-type spectrograph provided as an NST post-focus instrument through a collaboration between two Korean groups, Seoul National University (SNU) and Korean Astronomy and Space Institute (KASI). Lines typically observed by FISS are the Ca II H and K lines near 854 nm and the H α line. Both spectral regions can be observed simultaneously using a dual-camera system. The spectrograph slit is 40" long, and a field of view of 40" × 60" is typically scanned in 10 seconds. The H α camera is a 512 × 512 CCD, while the Ca II camera is a 1004 × 1000 CCD. The slit width is 32 μ m, which corresponds to a spatial sampling of 0.16". The spectral sampling at H α is typically 0.019 Å and at Ca II it is 0.025 Å, and the resolving power ($\lambda/\Delta\lambda = 1.4 \times 10^5$) gives a spectral resolution of 0.05 Å and 0.06 Å, respectively. The purpose of FISS is to study fast dynamics of solar features at moderate spatial resolution.

NST Cryogenic Infra-Red Spectrograph—Cyra

Cyra is still under development, and when completed will constitute a fully cryogenic, folded Czerny-Turner spectrograph based on a 2048 × 2048 HgCdTe array sensitive through the 1-5 μ m region. A correlation tracker is available for tip-tilt correction, and an image-rotator has been completed and is undergoing tests now. When complete, the system will include a rotating waveplate and polarizing beamsplitter for dual-beam, full-Stokes polarimetry. Test observations of the CO lines near 4667 nm (resolving power 250,000) have succeeded in showing off-limb emission. Photospheric lines of interest are Fe I 1565 nm, Ti I 2231 nm, Fe I 4064 nm, and Si I 4143 nm, while chromospheric lines are Ca I 3697 nm, Mg I 3682 nm, and the aforementioned CO lines. The instrument scan cadence will be a function of total integration time, number of Stokes parameters, and scanned field of view, but is expected to be under 1 min. The instrument is expected to be completed by 2017.

BBSO H α Full-Disk Imager

The H α full-disk patrol telescope is a 10 cm aperture refractor equipped with a Zeiss Lyot 0.025 nm bandpass filter with a tunable range of ± 0.3 nm. The detector size is 2048×2048 , 12-bit, for a spatial scale of about $1''/\text{pixel}$. The exposures are typically 30 ms, and frames are taken at a cadence of 1 frame/minute except during flares, when the cadence can be manually increased to 1 frame/15 seconds. The images are used in real time to aid in target selection of the NST, and are also used for context for the high-resolution NST data. In addition, the station is part of a world-wide network called the Global H α Network (GHN) comprising BBSO, Kanzelhöhe Solar Observatory in Germany, Catania Astrophysical Observatory in Italy, Meudon and Pic du Midi in France, Huairou and Yunnan Observatories in China, the Mauna Loa Solar Observatory in Hawaii, and the Uccle Solar Equatorial Table in Belgium.

BBSO GONG station

The BBSO operates on of the 6 GONG stations. A description of the instrumentation and capabilities of GONG is given in the NSO section at the beginning of this section (A.1).

A.2 Radio Facilities

National Radio Astronomy Observatory (VLA, VLBA, ALMA)

The **Very Large Array (VLA)** is a general purpose Fourier synthesis instrument comprised of 27 antennas, each 25 m in diameter. The antennas are distributed on three arms in a Y pattern in New Mexico. The antennas are reconfigurable into four standard configurations. In the largest configuration the antennas are spread over an area of 35 km (A configuration). In the most compact configuration they are distributed within 1 km (1 configuration). The angular resolution of a given configuration depends on its size. Hence, the (frequency-dependent) resolution of the VLA in the A configuration is $(1.75/\nu)$ and is roughly $(60''/\nu)$ in the D configuration, where ν is the frequency in GHz.

The VLA now operates over a frequency range of 1 – 50 GHz (6 mm to 30 cm) although the instantaneous bandwidth one can observe is an octave or less (e.g., 1 – 2, 2 – 4, 4 – 8 GHz, and so on). A given band is channelized to user-specified resolution, depending on science requirements. Full polarimetry is supported and integration times down to ≈ 10 ms are possible.

Imaging fidelity is related to the sampling density in Fourier space (the uv plane). Since the sun's radio brightness distribution is complex and variable, good instantaneous sampling is favored. The workhorse antenna configurations for VLA observations of the sun are the D configuration and the C configuration (3 km size). For studies of the corona

and solar wind using propagation techniques, the A configuration is best although there may be cases where the B configuration is needed (11 km size).

Like the VLA, the **Very Long Baseline Array (VLBA)** is a general purpose Fourier synthesis array. Unlike the VLA, it comprised of only 10 antennas, each 25 m in diameter. The antennas are fixed in position and are distributed from Hawaii to St. Croix in the Caribbean. It is used to perform very long baseline interferometry, essentially using the entire Earth as a telescope. It operates at frequencies ranging from \approx 1-100 GHz. With baselines up to 8000 km, it can achieve extraordinarily high degrees of angular resolution (e.g., 0.8 milliarcsec at 10 GHz). However, given the sparse sampling of the aperture it is not useful for imaging the sun. Moreover, scattering in the sun's corona strongly limits the angular resolution with which one can usefully imaging radio emission from the sun. Instead, the VLBA is useful for observing propagation phenomena such as phase and intensity scintillations in the solar wind.

The **Atacama Large Millimeter-submillimeter Array (ALMA)** is also a general purpose Fourier synthesis array, but it operates at much shorter wavelengths. Situated at an elevation of 5000 m in the Atacama desert in Chile, the array is comprised of 50 12 m antennas, 12 7-m antennas, and 4 total power antennas. It operates in ten frequency bands distributed from 84 – 950 GHz. While it was designed to carry out sensitive observations of cosmic dust and molecular gas, provisions were made to observe the sun. It is being commissioned for solar observing in 2015 – 16. ALMA will be able to observe thermal emission from the chromosphere at these frequencies, and will be sensitive to LOS chromospheric magnetic fields, with arcsecond angular resolution.

NJIT Owens Valley Solar Array (EOVSA)

The **Expanded Owens Valley Solar Array (EOVSA)** is a newly expanded, solar-dedicated radio interferometer consisting of 13 small, 2.1-m antennas (see Figure 3) for observing the sun and 2 large, 27-m antennas equipped with He-cooled receivers for calibration. The receivers are designed to cover the frequency range 1 – 18 GHz, although currently they operate from 2.5 – 18 GHz pending a modification to the design to eliminate debilitating radio frequency interference around 2 GHz. The 2.1-m antenna size is chosen to permit full-disk coverage of the sun at all frequencies, so that flares and active regions occurring anywhere on the sun will be within the field of view. The instrument processes radiation from the entire sun in the range 1 – 18 GHz each second and when the design modification to allow 1 – 18 GHz operation is complete, there will be 448 frequency channels available for scientific analysis. It is expected that the design modification will be completed by the time of the *Solar Probe Plus* and *Solar Orbiter* missions.